EurJIC European Journal of Inorganic Chemistry

ChemPubSoc Europe

FULL PAPER

DOI:10.1002/ejic.201201117

Two Members of the $\{X_4Nb_{16}O_{56}\}$ Family (X = Ge, Si) Based on $[(GeOH)_2Ge_2Nb_{16}H_2O_{54}]^{12-}$ and $[K(GeOH)_2Ge_2Nb_{16}H_3O_{54}]^{10-}$

CLUSTER ISSUE

Xin Zhang,[a] Shu-Xia Liu,*[a] Shu-Jun Li,[a] Yu-Huan Gao,[a] Xue-Na Wang,[a] Qun Tang,[a] and Yi-Wei Liu[a]

Keywords: Polyoxometalates / Polyoxoniobates / Niobium / Germanium / Photoluminescence / Electrochemistry

Two new heteropolyniobate compounds, $(C_2N_2H_{10})_6[(GeOH)_2Ge_2Nb_{16}H_2O_{54}]\cdot 25H_2O$ (**1**) and $[Cu(en)_2(H_2O)_2]_5K_{10}[K(GeOH)_2Ge_2Nb_{16}H_3O_{54}]_2\cdot 38H_2O$ (**2**, en = ethylenediamine), have been prepared under hydrothermal–conventional combination conditions and structurally characterized by elemental analysis, IR spectroscopy, powder and single-crystal XRD, diffuse reflection spectroscopy, and thermogravimetric (TG) analysis. Compounds **1** and **2** are based on $[(GeOH)_2Ge_2Nb_{16}H_2O_{54}]^{12-}$ and $[K(GeOH)_2Ge_2Nb_{16}H_3O_{54}]^{10-}$ building blocks, respectively. Compound **1** represents the initially isolated Nb/Ge lacunary derivative and compound **2** exhibits 1D ladderlike chains. The photoluminescence properties and electrochemical properties of compounds **1** and **2** have been investigated.

Introduction

Polyoxoniobates (PONs) are an important subclass of polyoxometalates (POMs), which not only exhibit structural diversity but also display multiple potential applications in virology, nuclear waste treatment, the base-catalyzed decomposition of biocontaminants, and photolysis of water to yield molecular hydrogen and oxygen.[1] Therefore, polyoxoniobates have attracted considerable attention and huge advances have been made in the past two decades. However, PON chemistry studies have focused on isopolyniobate chemistry, which is dominated by the Lindquist-type $[Nb_6O_{19}]^{8-}$ anions.[2,3] To date, heteropolyanion chemistry has been dominated by heteropolymolybdates, -tungstates, and -vanadates, which are usually prepared by precipitation from aqueous, acidified solutions at ambient temperature and pressure.[4] In contrast, heteropolyniobate compounds are less common and quite difficult to obtain in high yields. They are chiefly impeded by a lack of soluble precursors, the inertness of Nb species, the narrow window of the working pH range, and limited chemistry with most addenda metals.[5–7] Even so, several groups have been quite active in this area. The synthesis and structural characterization of a heteropolyanion-type compound $Na_{14}[H_2Si_4Nb_{16}O_{56}]\cdot 45.5H_2O$ was reported in 2002 by Nyman[8] and was a significant breakthrough in heteropolyoxoniobate chemistry. Subsequently, the Nyman and Cronin groups have reported many heteropolyoxoniobate compounds, such as $K_{12}[Ti_2O_2][SiNb_{12}O_{40}]\cdot 16H_2O$, $Na_{15}[(PO_2)_3PNb_9O_{34}]\cdot 22H_2O$, $Na_{16}[XNb_{12}O_{40}]\cdot 4H_2O$, $Na_{12}[Ti_2O_2][XNb_{12}O_{40}]\cdot nH_2O$, $Na_{10}[Nb_2O_2][XNb_{12}O_{40}]\cdot nH_2O$ (X = Si or Ge), and $[Cu(en)_2]_{3.5}[Cu(en)_2(H_2O)]\{[VNb_{12}O_{40}(VO)_2][Cu(en)_2]\}\cdot 17H_2O$ (en = ethylenediamine).[6,9–17] Our group has also recently made a deeper study on the reactivity of polyoxoniobates in acidic solutions and obtained some mixed-addendum heteropolyniobates.[18] Furthermore, Ge^{IV}-containing polyoxometalates have been known for several decades, and most of the published work was based on the Keggin-type germanotungstates $[GeW_{12}O_{40}]^{4-}$ and its lacunary derivatives.[19] In 1972, Choisnet et al. reported the Ge/Nb compound $RbNb(GeO_3)_3$, the first example of germanium introduced into a niobate.[20] In 2004, Nyman et al. reported the first Keggin germanoniobate $Na_{16}[GeNb_{12}O_{40}]\cdot 4H_2O$.[9] In recent years, several germanoniobate clusters have been reported, however, no more members of the $\{X_4Nb_{16}O_{56}\}$ family (X = Ge, Si) have been discovered.

Inspired by the aforementioned work, herein we report the synthesis, structure characterization, photoluminescence properties, and electrochemical activity of two new heteropolyoxoniobates, $(C_2N_2H_{10})_6[(GeOH)_2Ge_2Nb_{16}H_2O_{54}]\cdot 25H_2O$ (**1**) and $[Cu(en)_2(H_2O)_2]_5K_{10}[K(GeOH)_2Ge_2Nb_{16}H_3O_{54}]_2\cdot 38H_2O$ (**2**), in which the polyoxoanion clusters are the latest members of the $\{X_4Nb_{16}O_{56}\}$ family (X = Ge, Si). Large single crystals of these compounds have been successfully synthesized in high yield and characterized by elemental analysis, powder XRD

[a] Key Laboratory of Polyoxometalate Science of the Ministry of Education, College of Chemistry, Northeast Normal University,
Changchun, Jilin 130024, China
Fax: +86-431-85099328
E-mail: liusx@nenu.edu.cn

Supporting information for this article is available on the WWW under http://dx.doi.org/10.1002/ejic.201201117.

(PXRD), IR spectroscopy, diffuse reflection spectroscopy, single-crystal XRD, and thermogravimetric analyses. To the best of our knowledge, compound **1** represents the first example of an isolated Ge/Nb lacunary derivative, the structure type of which has been previously observed only in a Si/Nb heteropoly compound,[8] and compound **2** is a new sandwich-type germanoniobate, in which two $[K(GeOH)_2Ge_2Nb_{16}H_3O_{54}]^{10-}$ units sandwich eight potassium ions in the central belt.

Results and Discussion

Synthesis

Compounds **1** and **2** were synthesized by adopting a hydrothermal–conventional combination approach. Compound **1** was synthesized by slow evaporation of the mother liquor after the hydrothermal reaction of $K_7HNb_6O_{19}\cdot 13H_2O$, GeO_2, $N_2H_4\cdot H_2SO_4$, and en in H_2O. Owing to the stability of niobium radical species, the intention of our experiments was to find a strong reducing agent to take advantage of the valence variation at high temperature and pressure. However, the results were not as we expected. This compound was also obtained without $N_2H_4\cdot H_2SO_4$. Compound **1** is insoluble in water and some organic solvents (C_2H_5OH, CH_2Cl_2, CH_3CN) at room temperature. Compound **2** was obtained by means of a singular synthetic strategy, in which $CuSO_4\cdot 5H_2O$ and KOH were added to clarify the mother liquor before the formation of **1**. In our experiments, we have constantly tried to replace Cu^{2+} with other transition metal ions, such as Co^{2+}, Zn^{2+}, and Ni^{2+}, but single-crystal samples were not obtained. A great many tentative experimental results show that the alkali metal cations (K^+) play a vital role in the formation of **2**. This means that **2** cannot form only in the presence of copper countercations. Unlike sandwich-type heteropolytungstates and -molybdates, it is observed that potassium cations rather than transition metal cations occupy the lacunary sites in the structure of compound **2**. This may be due to the steric effect of the copper/en complex. Moreover, control of the evaporation temperature plays an important role in definite crystal formation of compound **2**; when the other conditions remained unchanged, a bluish purple precipitate formed at room temperature. Therefore, we performed the crystallization at low temperature, and good single-crystal products were obtained in high yield. Furthermore, compound **2** is water soluble, unlike compound **1**.

Crystal Structures of 1 and 2

Single-crystal X-ray diffraction structural analyses reveal that the entire structure of compound **1** is constructed from new polyoxoanions $[(GeOH)_2Ge_2Nb_{16}H_2O_{54}]^{12-}$ and diprotonated ethylenediamine (enH_2^{2+}) serves as the charge-compensating cations. The structure of $[(GeOH)_2Ge_2Nb_{16}H_2O_{54}]^{12-}$ is shown in Figure 1. The NbO_6 octahedra can be split into two sorts, two Nb_3O_{13} unit that are triplets of edge-sharing NbO_6 octahedra and two Nb_5O_{17} units that are quintets of edge-sharing NbO_6 octahedra. These two sets are then linked together by corner-sharing to give a "wupeng boat" arrangement. Two trimetal clusters are the bow and stern, and two pentametal clusters form the bottom and hull of the boat (Figure S1 in the Supporting Information). Each niobium atom has a distorted $\{NbO_6\}$ octahedral environment, and the Nb–O bond distances can be subdivided into three groups: Nb–O_c (O_c, Nb–O_c–Ge bridging O atoms), 2.143(1)–2.414(9) Å; Nb–O_b (O_b, Nb–O_b–Nb bridging O atoms), 1.872(7)–2.147(6) Å; and Nb–O_t (O_t, terminal O atoms), 1.756(0)–1.790(3) Å. Two of the four GeO_4 tetrahedra are encapsulated in the cabin of the boat, which gives rise to a heteropolyanion centered about a Ge_2O_7 (Ge1, Ge2) dimer. This structure centered about P_2O_7 and Si_2O_7 dimers has been heretofore observed in literature.[4d,4e,8] The Ge_2O_7 dimer has Ge–O distances of 1.722(6)–1.769(8) Å, and the average Ge–O bond length for both these interior GeO_4 tetrahedra is 1.752(7) Å. The Ge1–O–Ge2 bond angle (Ge_2O_7 dimer) is 119.398(32)°. The other two GeO_4 tetrahedra are located on the cabin (lacunary site) of the boat, and the distances of the Ge–O bonds can be divided into two groups: Ge–O_c (O_c, Ge–O_c–Nb bridging O atoms), 1.710(3)–1.766(1) Å and Ge–O_t (O_t, terminal O atoms), 1.769(2)–1.784(6) Å. Furthermore, bond valence sums (BVS) for niobium, germanium, and oxygen atoms were calculated by using the parameters given by Brown,[21] which showed that all the Nb and Ge atoms remain in their highest oxidation states, and could also mean that the Nb species have low activity. The BVS values of 0.996 and 1.004 for O55 and O56 (terminal oxygen atoms of GeO_4) indicate they are actually monoprotonated.

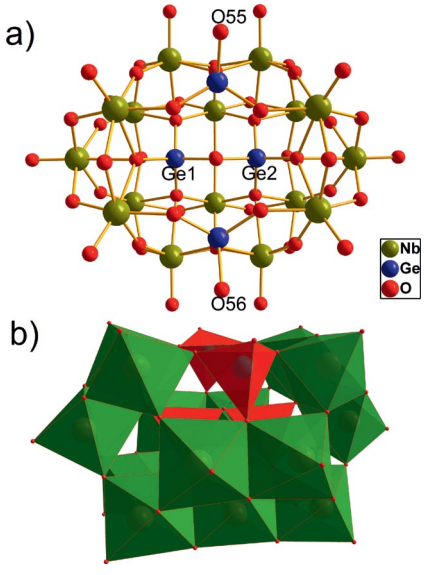

Figure 1. Ball-and-stick representation (a) and polyhedral representation (b) of the $[(GeOH)_2Ge_2Nb_{16}H_2O_{54}]^{12-}$ polyanion in **1**. Octahedra: NbO_6, tetrahedra: GeO_4; All H atoms are omitted for clarity.

The asymmetric unit of **1** can also be derived formally from the archetypal spherical Keggin skeleton $\{GeNb_{12}\}$.

The geometrical arrangement of the $[(GeOH)_2Ge_2Nb_{16}H_2O_{54}]^{12-}$ cluster may be described as a combination of two three-vacancy Keggin ions by corner-sharing of their linear triad of octahedra. These two Keggin ions share two NbO_6 octahedra, and the other two GeO_4 tetrahedra are added to the $[Ge_2Nb_{16}H_2O_{54}]^{18-}$ anion by rational self-assembly.

The structure of **2** was determined by single-crystal X-ray diffraction analysis and consists of two $[K(GeOH)_2Ge_2Nb_{16}H_3O_{54}]^{10-}$ secondary building units linked by eight potassium atoms to form a dimer that is charge-balanced by five $[Cu(en)_2(H_2O)_2]^{2+}$ complexes. This dimeric structure can be seen as a sandwich-type configuration, in which eight K atoms are combined with two $[K(GeOH)_2Ge_2Nb_{16}H_3O_{54}]^{10-}$ subunits through eight exposed terminal O atoms (as shown in Figure 2). It is worth noting that the $[K(GeOH)_2Ge_2Nb_{16}H_3O_{54}]^{10-}$ cluster has idealized D_{2h} symmetry. Compared to the $[(GeOH)_2Ge_2Nb_{16}H_2O_{54}]^{12-}$ polyanion, a single potassium atom exists in the "pocket" (lacunary site) of the polyanionic $[K(GeOH)_2Ge_2Nb_{16}H_3O_{54}]^{10-}$. The pocket potassium atom (K1) is connected to six oxygen atoms, four of which are from the NbO_6 octahedra and GeO_4 tetrahedra, and the other two are from water molecules. The K1–O_b (O_b, Nb–O_b–Ge bridging O atoms) bond lengths are 2.380(6) Å and the two K1–O_w (w = water) bond lengths are 2.462(2) Å. These water molecules bridge the two K1 sites of the dimer and link the two $[K(GeOH)_2Ge_2Nb_{16}H_3O_{54}]^{10-}$ subunits together. Compared with compound **1**, the coordination of the K1 atom results in the slight distortion of the NbO_6 octahedron attached to the K1 atom (see Figure S2 and Table S1 in the Supporting Information). The center gap of the dimer also contains eight more potassium atoms including four K2 atoms and four K4 atoms. The K2 atoms link to two $[K(GeOH)_2Ge_2Nb_{16}H_3O_{54}]^{10-}$ units through two Nb–O_t–K bridges. The K4 atoms also link to two $[K(GeOH)_2Ge_2Nb_{16}H_3O_{54}]^{10-}$ subunits and also coordinate to three O_w atoms. A similar anion $[Na(SiOH)_2Si_2Nb_{16}H_{3.5}O_{54}]_2^{19-}$ has been previously reported with $[Cu(en)_2(H_2O)_2]^{2+}$ and Na^+ countercations.[22] In this anion, a $\{Na_2Ow_2\}$ segment replaces the $\{K_2Ow_2\}$ segment in **2** that associates the two $\{Na(SiOH)_2Si_2Nb_{16}H_{3.5}O_{54}\}$ units into a dimer. In the central belt of the two $\{Na(SiOH)_2Si_2Nb_{16}H_{3.5}O_{54}\}$ units, there are another five Na atoms, which adopt different arrangements to those of K2 and K4 in **2**. For this dimer, there are five $[Cu(en)_2(H_2O)_2]^{2+}$ fragments situated freely around the cluster to balance the charge of the entire structure. Each $[Cu(en)_2(H_2O)_2]^{2+}$ group has Cu–N bond lengths of 1.995(3) to 2.004(5) Å, and the axial Cu–O_w bond distances range from 2.555(0) to 2.590(4) Å. Moreover, the $[K(GeOH)_2Ge_2Nb_{16}H_3O_{54}]^{10-}$-polyoxoanion dimers are linked to each other by a μ-K atom to construct 1D ladderlike chains along the *b* axis (Figure 3). BVS calculations confirm that the oxidation state of copper is +2. Similar to those for compound **1**, BVS calculations for **2** also give BVS values of 1.017 for O5 (terminal oxygen of GeO_4), which further indicate the protonation positions [Figure S2(b) in the Supporting Information]. More interestingly, this 1D ladder-type chain of alternating self-assembled layers forms a 2D network (Figure S3 in the Supporting Information).

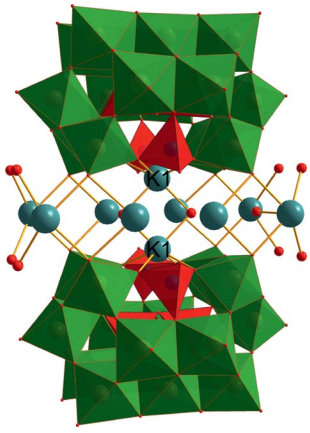

Figure 2. Mixed polyhedral and ball-and-stick representation of the $[K(GeOH)_2Ge_2Nb_{16}H_3O_{54}]_2^{20-}$ polyanion in **2**. Octahedra: NbO_6, tetrahedra: GeO_4, teal spheres: K, red spheres: O. All H atoms are omitted for clarity.

Charge-balance considerations for **1** and **2** demand that there must be extra protons in the $\{(GeOH)_2Ge_2Nb_{16}\}$ and $\{K(GeOH)_2Ge_2Nb_{16}\}$ units. As explained by Nyman, the very high number of crystallographically independent atoms and variable parameters prevents the determination

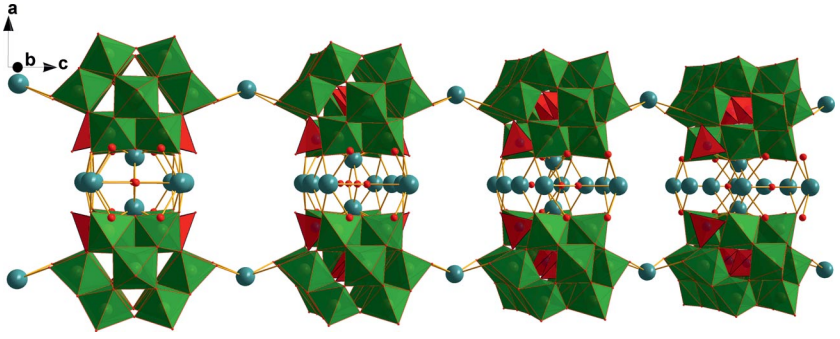

Figure 3. View of the 1D ladderlike chain of **2**, projected approximately down the *b* axis. Octahedra: NbO_6, tetrahedra: GeO_4, teal spheres: K, red spheres: O. The $[Cu(en)_2(H_2O)_2]^{2+}$ and part of the coordinated water molecules are omitted for clarity.

of the exact location of the protons from the Fourier maps, and even bond-valence calculations do not provide an obvious position for the protons.[2c,7] Therefore, we hypothesize that the most reasonable location may be that these charge-balancing protons are disordered over bridging μ_2-ONb_2 sites of the cluster.[22,23] In **1**, the uncoordinated diprotonated enH_2^{2+} cations serve as the counterions to balance the negative charges from the $[(GeOH)_2Ge_2Nb_{16}H_2O_{54}]^{12-}$ ion. It is worth noting that the anions in **1** are charge balanced by protonated organic species, which is quite atypical for polyoxoniobates. These facts suggest that the organic cations can provide new avenues towards diversification of polyoxoniobate cluster geometries.[7] Moreover, we find that en also acts as a structure-directing agent in the formation of the specific polyoxoniobates clusters, because no single crystal were obtained in the absence of en or if en was replaced. In **2**, in addition to five $[Cu(en)_2(H_2O)_2]^{2+}$ fragments, additional potassium atoms act as counterbalance cations for each sandwich-type cluster unit.

Powder XRD and IR Spectra

The experimental PXRD patterns of **1** and **2** are in good agreement with the simulated patterns, which indicates the phase purity of the samples (Figure S4 in the Supporting Information). The intensity difference between the experimental and simulated PXRD patterns is attributed to the variation in the preferred orientation of the powder sample during collection of the experimental pattern.

The compositional analyses for **1** and **2** were not only carried out by elemental analyses, but were also confirmed by the IR analyses (Figure S5 in the Supporting Information). In the IR spectrum of **1**, the CH_2 and NH_2 stretching bands are observed at $\tilde{\nu}$ = 3014 to 3231 and 1156 to 1616 cm^{-1}, respectively, and their bending bands are observed at $\tilde{\nu}$ = 1507 to 1615 and 1322 to 1456 cm^{-1}, respectively. These signals confirm the presence of amino groups. The characteristic peaks at $\tilde{\nu}$ = 1057, 988, 920, 854, 688, and 518 cm^{-1} are assigned to the $\nu(M–O_t)$, $\nu(Ge–O_c)$, and $\nu(M–O_b–M)$ stretches (M = Nb^V or Ge^{IV}). The peak at$\tilde{\nu}$ = 3405 cm^{-1} is assigned to the water molecules. The IR spectrum of **2** additionally has the signals of amino groups, and the characteristic peaks at $\tilde{\nu}$ = 1052, 921, 864, 754, 695, and 523 cm^{-1} are assigned to the $\nu(M–O_t)$, $\nu(Ge–O_c)$, and $\nu(M–O_b–M)$ stretches. The broad band at $\tilde{\nu}$ = 3409 cm^{-1} is ascribed to the O–H vibrations from the water molecules. All these results are consistent with the X-ray single-crystal structural analysis.

UV/Vis Diffuse Reflectance Spectra and Photoluminescence

The UV/Vis diffuse reflectance spectra of **1** and **2** show intense absorption bands in the range 200 to 400 nm with one main band at ca. 248 and 247 nm, respectively. These are mainly attributed to oxide-to-metal (O→Nb) charge-transfer (OMCT) transitions.[24] A wide absorption at ca. 550 nm for **2** can be ascribed to the d–d transition ($^2B_{1g}\rightarrow{}^2B_{2g}$) and the ligand-to-metal charge-transfer (LMCT, $\pi_\sigma^*\rightarrow d_{xy}$) in $[Cu(en)_2(H_2O)_2]^{2+}$ (Figure 4).[25]

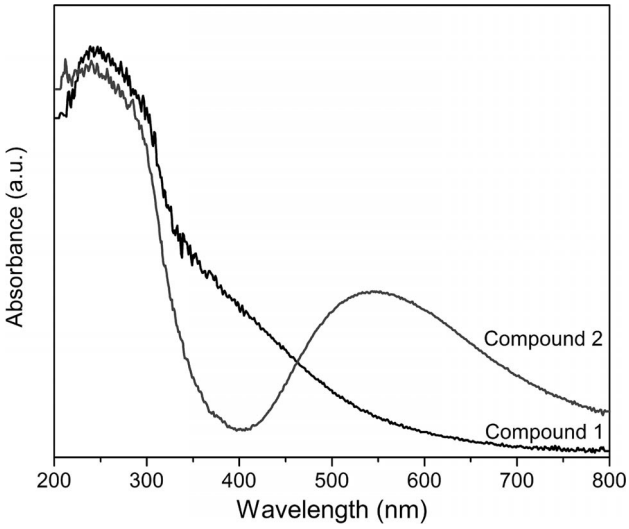

Figure 4. The UV/Vis diffuse reflectance spectra of **1** and **2**.

The luminescence of the niobate group has been investigated extensively in crystal materials and is strongly dependent upon the crystal structure.[26] Niobate luminescence is affected by the configuration of the NbO_6 octahedron, the coordination symmetry of the metal atoms, or the participation of alkali metal atoms.[27] Isolated and edge- or face-shared NbO_6 octahedral groups show efficient luminescence owing to delocalization of the excited state.[26a] The photoluminescence spectra of **1** and **2** were measured (Figure S6 in the Supporting Information). As we anticipated, the optical properties of the polyoxoniobates change owing to structural changes and the participation of alkali metal atoms. The broad emission band has its maximum at 441 nm with the corresponding excitation band at 371 nm for **1**, and the emission band has its maximum at 418 nm with the corresponding excitation band at 347 nm for **2**. We speculate that this difference may be due to alkali-metal coordination, which distorts the NbO_6 octahedron, and the difference in symmetry results in slight changes to their fluorescence emission spectra. The emission bands at 441 and 418 nm may be attributed to the distorted NbO_6 octahedra.[26b]

Thermogravimetric Analysis

The thermogravimetric analyses (TGA) of **1** and **2** were conducted with crystalline samples under a nitrogen atmosphere from 25 to 600 °C (Figure S7 in the Supporting Information). We found that the TG curves of **1** and **2** both exhibit two weight-loss steps. For **1**, the first weight-loss step corresponds to the loss of lattice water molecules (13.0%, calcd. 12.93%) in the range 25–260 °C. The second weight loss step was attributed to the loss of diprotonated organic en molecules (10.5%, calcd. 11.13%) in the range

270–560 °C. For **2**, the first weight-loss step corresponded to the loss of lattice and coordinated water molecules (11.5%, calcd. 11.52%) in the range 25–270 °C. The second weight-loss step was ascribed to the loss of organic en molecules (7.52%, calcd. 8.01%) in the range 260–560 °C. These observations indicate that the experimental values are approximately consistent with the theoretical values.

Electrochemistry

The electrochemical activity of **1** was studied in 0.2 M Na_2SO_4, and that of **2** (0.5 mM) was studied in an electrolyte solution of 0.2 M KNO_3. In the potential range –1000 to 1000 mV (scan rate: 100 mV s^{-1}), no redox wave was observed in the cyclic voltammogram of **1**. Similarly, no niobium redox processes were observed for compound **2**, and it only exhibits the electrochemical character of copper–en complex cations. In the cyclic voltammogram of **2** at a scan rate of 100 mV s^{-1} (Figure S8), two reduction peaks appear at –87.5 and –144.5 mV, and their oxidation counterpart (a single oxidation process) is located at +71.5 mV. These peaks are attributed to the redox processes of the Cu^{2+} centers, and the pattern features the two-step reduction of Cu^{2+} to Cu^0 through Cu^{1+}.[28] Taking the oxidation peak as representative, when the scan rate varied from 20 to 600 mV s^{-1}, the peak currents are proportional to the square root of the scan rates, which indicates that the procedure is controlled by diffusion (inset of Figure S9). With increasing scan rate, the oxidation peak potential shifted slightly positively, and the reduction peak potential shifted slightly negatively (Figure S9).

Conclusions

In this work, two new heteropolyniobate clusters based on $[(GeOH)_2Ge_2Nb_{16}H_2O_{54}]^{12-}$ and $[K(GeOH)_2Ge_2Nb_{16}H_3O_{54}]^{10-}$ polyoxoanions have been synthesized by a hydrothermal–conventional combination approach. Elemental analysis, IR spectroscopy, powder and single-crystal XRD, diffuse reflection spectroscopy, and TGA reveal the structural characteristics of the two clusters. Compound **1** is an isolated cluster and compound **2** is a sandwich-type germanoniobate in which two $[K(GeOH)_2Ge_2Nb_{16}H_3O_{54}]^{10-}$ units sandwich eight potassium atoms in the central belt. The dimeric units bridge each other through a μ-K atom to result in the extended structure. The present study introduces Ge into the $\{X_4Nb_{16}O_{56}\}$ family (X = Ge, Si) for the first time and provides two new members of the family, which has been known for ten years. The successful preparation of these heteropolyniobates provides a synthetic route for the exploration of new high-nuclear polyoxoniobate backbones and further guides the rational assembly with addenda metals to produce new multifunctional PON hybrids.

Experimental Section

Materials, Methods, and Instrumentation: All reagents except $K_7HNb_6O_{19}\cdot13H_2O$ were purchased from commercial sources and used without further purification. The $K_7HNb_6O_{19}\cdot13H_2O$ precursors were synthesized according to procedures described in the literature[29] and were characterized by IR spectroscopy. IR spectroscopy was performed in the range 4000–400 cm^{-1} by using KBr pellets with an Alpha Centauri FT/IR spectrophotometer. Elemental analyses for K, Nb, Ge, Cu, C, and N were determined with a PLASMASPEC (I) inductively coupled plasma (ICP) atomic emission spectrometer. Powder XRD measurements were recorded from 5 to 50° at room temperature with a Siemens D5005 diffractometer with Cu-K_α (λ = 1.5418 Å) radiation. TGA of the samples was performed with a Perkin–Elmer TG-7 analyzer heated from room temperature to 600 °C under nitrogen at a heating rate of 10 °C min^{-1}. UV/Vis diffuse reflectance spectra (UV/Vis/DRS) were recorded with a Cary 500 UV/Vis/NIR spectrometer. The photoluminescent properties were measured with an FLSP920 Edinburgh fluorescence spectrometer. Electrochemical measurements were performed with a CHI660B electrochemical workstation (Chenhua Instruments Co., Shanghai, China). A three-electrode system was employed in this study. A carbon paste electrode (CPE) and a glassy carbon electrode were used as the working electrode, an Ag/AgCl electrode as the reference electrode, and a Pt coil as a counterelectrode. A **1**-modified carbon paste electrode (1-CPE) was used as the working electrode and was prepared as follows: graphite powder (100 mg) and compound **1** (10 mg) were mixed and ground together with an agate mortar and pestle to achieve a homogeneous mixture, and then atolein (0.15 mL) was added with stirring. The mixture was packed into a small glass tube, and the tube surface was wiped with weighing paper. Electrical contact was established with a copper rod through the back of the electrode.[30] All the experiments were conducted at ambient temperature (25–30 °C).

$(C_2N_2H_{10})_6[(GeOH)_2Ge_2Nb_{16}H_2O_{54}]\cdot25H_2O$ (1): $K_7HNb_6O_{19}\cdot13H_2O$ (0.20 g, 0.15 mmol) and GeO_2 (0.09 g, 0.86 mmol) were combined in deionized water (10 mL), and $N_2H_4\cdot H_2SO_4$ (0.05 g, 0.38 mmol) and en (0.5 mL) were added with continuous stirring. The mixture was stirred for 10 min and placed in a 23 mL Teflon liner for a Parr reactor at 200 °C for 24 h, which resulted in a clear solution after the mixture was cooled to room temperature. Slow evaporation of the solution in air resulted in the formation of block-shaped colorless crystals after 5 d. The crystals were collected by filtration and air-dried. Yield: 55 mg (69.5% based on Nb). $C_{12}H_{114}Ge_4N_{12}Nb_{16}O_{81}$ (3499.93): calcd. C 4.12, H 3.28, Ge 8.30, N 4.80, Nb 42.47; found C 4.13, H 3.24, Ge 8.34, N 4.82, Nb 42.69.

$[Cu(en)_2(H_2O)_2]_5K_{10}[K(GeOH)_2Ge_2Nb_{16}H_3O_{54}]_2\cdot38H_2O$ (2): The synthetic procedure was similar to that for **1**. A clear solution formed after the hydrothermal reaction was performed without $N_2H_4\cdot H_2SO_4$. $CuSO_4\cdot5H_2O$ (0.05 g, 0.2 mmol) and KOH (0.01 g, 0.18 mmol) were added to the clear solution with stirring, and the mixture was heated to 100 °C. The pH of the precursor mixture was about 12.5. After 4–5 d at 10 °C, slow evaporation of the blue solution in air led to the formation of blue block-shaped crystals. These crystals were collected by filtration and air-dried. Yield: 45 mg (81.8% based on **1**). The estimated formula of **2** is $[Cu(en)_2(H_2O)_2]_5K_{10}[K(GeOH)_2Ge_2Nb_{16}H_3O_{54}]_2\cdot38H_2O$ (7501.78): calcd. C 3.23, H 2.25, Cu 4.28, Ge 7.82, N 3.77, Nb 40.02 K 6.32; found C 3.16, H 2.46, Cu 4.18, Ge 7.64, K 6.17, N 3.68, Nb 39.07.

X-ray Crystallography: Crystal data for compounds **1** and **2** were collected with Bruker APEX-II CCD detector with graphite monochromatic Mo-K_α radiation (λ = 0.71073 Å) at 296(2) K. The linear absorption coefficients, scattering factors for the atoms, and anomalous dispersion corrections were taken from the International Tables for X-ray Crystallography.[31] Empirical absorption correc-

Table 1. Crystal data and structural refinement for compounds **1** and **2**.

	1	**2**
Formula	$C_{12}H_{114}N_{12}Ge_4Nb_{16}O_{81}$	$C_{20}H_{106}N_{20}K_{12}Cu_5Ge_8Nb_{32}O_{160}$
Formula weight [g mol^{-1}]	3499.93	7501.78
T [K]	296	293
Wavelength [Å]	0.71073	0.71073
Crystal system	anorthic	orthorhombic
Space group	$P\bar{1}$	*Immm*
a [Å]	13.8766(1)	25.8594(8)
b [Å]	14.2573(1)	30.3591(10)
c [Å]	21.7048(1)	15.1186(5)
α [°]	90.792(1)	90
β [°]	98.758(1)	90
γ [°]	98.506(1)	90
V [Å^3]	4194.5(5)	11869.1(7)
Z	2	2
$D_{calcd.}$ [mg m^{-3}]	2.646	2.099
μ [mm^{-1}]	3.625	3.215
F(000)	3192.0	7122.0
Crystal size [mm]	0.20 × 0.18 × 0.18	0.20 × 0.18 × 0.18
Goodness-of-fit on F^2	1.042	1.072
Final R indices [$I > 2\sigma(I)$][a]	R_1 = 0.0469, wR_2 = 0.1217	R_1 = 0.0533, wR_2 = 0.1525
R indices[a] (all data)	R_1 = 0.0701, wR_2 = 0.1344	R_1 = 0.0720, wR_2 = 0.1639

[a] $R_1 = \Sigma||F_o| - |F_c||/\Sigma|F_o|$; $wR_2 = \{\Sigma[w(F_o^2 - F_c^2)^2]/\Sigma[w(F_o^2)^2]\}^{1/2}$.

tions were applied. Both structures were solved by direct methods and refined by full-matrix least-squares on F^2 by using the SHELXTL–97 program.[32] Anisotropic thermal parameters were used to refine all non-hydrogen atoms except for several oxygen and carbon atoms. Positions of the hydrogen atoms attached to carbon atoms were fixed at their ideal positions, and those hydrogen atoms attached to lattice water molecules were not located. Crystallization water molecules were estimated by thermogravimetry and only partial oxygen atoms of the water molecules were located with the X-ray structure analysis. A summary of the crystallographic data and structure refinement results of **1** and **2** are presented in Table 1.

CCDC-899400 (for **1**) and -899401 (for **2**) contain the supplementary crystallographic data for this paper. These data can be obtained free of charge from The Cambridge Crystallographic Data Centre via www.ccdc.cam.ac.uk/data_request/cif.

Supporting Information (see footnote on the first page of this article): Additional structural figures and tables, powder XRD patterns, IR spectra, TG curves, and photoluminescence spectra.

Acknowledgments

This work was supported by the National Natural Science Foundation of China (NSFC) (grant numbers 21171032 and 21231002), the Fundamental Research Funds for the Central Universities (grant numbers 09ZDQD0015 and 10SSXT136), and the Open Research Fund of the State Key Laboratory of Inorganic Synthesis and Preparative Chemistry (Jilin University, grant number 2012-10).

[1] a) J. T. Rhule, C. L. Hill, D. A. Judd, *Chem. Rev.* **1998**, *98*, 327; b) F. E. Osterloh, *Chem. Mater.* **2008**, *20*, 35; c) Z.-Y. Zhang, Q.-P. Lin, D. Kurunthu, T. Wu, F. Zuo, S.-T. Zheng, C. J. Bardeen, X.-H. Bu, P.-Y. Feng, *J. Am. Chem. Soc.* **2011**, *133*, 6934; d) M. H. Chiang, C. W. Williams, L. Soderhlm, M. R. Antonio, *Eur. J. Inorg. Chem.* **2003**, *14*, 2663; e) U. Kortz, M. G. Savelieff, B. S. Bassil, B. Keita, L. Nadjo, *Inorg. Chem.* **2002**, *41*, 783; f) A. Besserguenew, M. Dickman, M. Pope, *Inorg. Chem.* **2001**, *40*, 2582; g) M. Nyman, *Dalton Trans.* **2011**, *40*, 8049.

[2] a) E. M. Villa, C. A. Ohlin, E. Balogh, T. M. Anderson, M. Nyman, W. H. Casey, *Angew. Chem.* **2008**, *120*, 4922; *Angew. Chem. Int. Ed.* **2008**, *47*, 4844; b) J.-Y. Niu, G. Wang, J.-W. Zhao, Y.-X. Sui, P.-T. Ma, J.-P. Wang, *Cryst. Growth Des.* **2011**, *11*, 1253; c) J.-Y. Niu, P.-T. Ma, H.-Y. Niu, J. Li, J.-W. Zhao, Y. Song, J.-P. Wang, *Chem. Eur. J.* **2007**, *13*, 8739; d) M. Maekawa, Y. Ozawa, A. Yagasaki, *Inorg. Chem.* **2006**, *45*, 9608.

[3] I. Lindqvist, *Ark. Kemi* **1953**, *5*, 247.

[4] a) U. Kortz, M. G. Savelieff, F. Y. Abou Ghali, L. M. Khalil, S. A. Maalouf, D. Sinno, *Angew. Chem.* **2002**, *114*, 4246; *Angew. Chem. Int. Ed.* **2002**, *41*, 4070; b) X.-Y. Wei, M. H. Dickman, M. T. Pope, *J. Am. Chem. Soc.* **1998**, *120*, 10254; c) Y. V. Geletii, C. L. Hill, R. H. Atalla, I. A. Weinstock, *J. Am. Chem. Soc.* **2006**, *128*, 17033; d) U. Kortz, *Inorg. Chem.* **2000**, *39*, 623; e) U. Kortz, M. T. Pope, *Inorg. Chem.* **1994**, *33*, 5643; f) Y.-G. Wei, M. Lu, C. F. Cheung, C. L. Barnes, Z.-H. Peng, *Inorg. Chem.* **2001**, *40*, 5489; g) S.-X. Liu, D.-H. Li, L.-H. Xie, H.-Y. Cheng, X.-Y. Zhao, Z.-M. Su, *Inorg. Chem.* **2006**, *45*, 8036.

[5] J.-Y. Niu, G. Chen, J.-W. Zhao, P.-T. Ma, S.-Z. Li, J.-P. Wang, M.-X. Li, Y. Bai, B.-S. Ji, *Chem. Eur. J.* **2010**, *16*, 7082.

[6] Y. Hou, M. Nyman, M. A. Rodriguez, *Angew. Chem.* **2011**, *123*, 12722; *Angew. Chem. Int. Ed.* **2011**, *50*, 12514.

[7] R. P. Bontchev, M. Nyman, *Angew. Chem.* **2006**, *118*, 6822; *Angew. Chem. Int. Ed.* **2006**, *45*, 6670.

[8] M. Nyman, F. Bonhomme, T. M. Alam, M. A. Rodriguez, B. R. Cherry, J. L. Krumhansl, T. M. Nenoff, A. M. Sattler, *Science* **2002**, *297*, 996.

[9] M. Nyman, F. Bonhomme, T. M. Alam, J. B. Parise, G. M. B. Vaughan, *Angew. Chem.* **2004**, *116*, 2847; *Angew. Chem. Int. Ed.* **2004**, *43*, 2787.

[10] F. Bonhomme, J. P. Larentzos, T. M. Alam, E. J. Maginn, M. Nyman, *Inorg. Chem.* **2005**, *44*, 1774.

[11] M. Nyman, A. J. Celestian, J. B. Parise, G. P. Holland, T. M. Alam, *Inorg. Chem.* **2006**, *45*, 1043.

[12] M. Nyman, J. P. Larentzos, E. J. Maginn, M. E. Welk, D. Ingersoll, H. Park, J. B. Parise, I. Bull, F. Bonhomme, *Inorg. Chem.* **2007**, *46*, 2067.

[13] Z.-Y. Zhang, Q.-P. Lin, D. Kurunthu, T. Wu, F. Zuo, S.-T. Zheng, C. J. Bardeen, X.-H. Bu, P.-Y. Feng, *J. Am. Chem. Soc.* **2011**, *133*, 6934.
[14] T. M. Anderson, S. G. Thoma, F. Bonhomme, M. A. Rodriguez, Park, J. B. Parise, T. M. Alam, J. P. Larentzos, M. Nyman, *Cryst. Growth Des.* **2007**, *7*, 719.
[15] C. A. Ohlin, E. M. Villa, J. C. Fettinger, W. H. Casey, *Angew. Chem.* **2008**, *120*, 5716; *Angew. Chem. Int. Ed.* **2008**, *47*, 5634.
[16] G.-L. Guo, Y.-Q. Xu, J. Cao, C.-W. Hu, *Chem. Commun.* **2011**, *47*, 9411.
[17] P. Huang, C. Qin, X.-L. Wang, C.-Y. Sun, G.-S. Yang, K.-Z. Shao, Y.-Q. Jiao, K. Zhou, Z.-M. Su, *Chem. Commun.* **2012**, *48*, 103.
[18] a) S.-J. Li, S.-X. Liu, C.-C. Li, F.-J. Ma, D.-D. Liang, W. Zhang, R.-K. Tan, Y.-Y. Zhang, L. Xu, *Chem. Eur. J.* **2010**, *16*, 13435; b) S.-J. Li, S.-X. Liu, N.-N. Ma, Y.-Q. Qiu, J. Miao, C.-C. Li, Q. Tang, L. Xu, *CrystEngComm* **2012**, *14*, 1397; c) C.-C. Li, S.-X. Liu, S.-J. Li, Y. Yang, H.-Y. Jin, F.-J. Ma, *Eur. J. Inorg. Chem.* **2012**, *19*, 3229.
[19] a) H. Katano, T. Osakai, S. Himeno, A. Saito, *Electrochim. Acta* **1995**, *40*, 2935; b) J.-F. Liu, B.-L. Zhao, C.-Y. Rong, M. T. Pope, *Acta Chim. Sin. (Engl. Ed.)* **1993**, *51*, 368; c) L. Meng, J.-F. Liu, *Chin. J. Chem.* **1995**, *13*, 334; d) N. H. Nsouli, B. S. Bassil, M. H. Dickman, U. Kortz, B. Keita, L. Nadjo, *Inorg. Chem.* **2006**, *45*, 3858; e) J.-W. Zhao, J. Zhang, Y. Song, S.-T. Zheng, G.-Y. Yang, *Eur. J. Inorg. Chem.* **2008**, *24*, 3809.
[20] J. Choisnet, A. Deschanvres, B. Raveau, *J. Solid State Chem.* **1972**, *4*, 209.
[21] I. D. Brown, D. Altermatt, *Acta Crystallogr., Sect. B* **1985**, *41*, 244.
[22] T. M. Anderson, T. M. Alam, M. A. Rodriguez, J. N. Bixler, W.-Q. Xu, J. B. Parise, M. Nyman, *Inorg. Chem.* **2008**, *47*, 7834.
[23] T. Ozeki, T. Yamase, H. Naruke, Y. Sasaki, *Bull. Chem. Soc. Jpn.* **1994**, *67*, 3249.
[24] a) E. Papaconstantinou, *Chem. Soc. Rev.* **1989**, *18*, 1; b) C. Streb, *Dalton Trans.* **2012**, *41*, 1651.
[25] a) A. T. Baker, *J. Chem. Educ.* **1998**, *75*, 98; b) L. M. Mirica, X. Ottenwaelder, T. D. P. Stack, *Chem. Rev.* **2004**, *104*, 1013; c) O. Z. Yeşilel, İ. İlker, M. S. Soylu, C. Darcan, Y. Süzen, *Polyhedron* **2012**, *39*, 14; d) G. Ramadevudu, M. Shareefuddin, N. S. Bai, M. L. Rao, M. N. Chary, *J. Non-Cryst. Solids* **2000**, *278*, 205.
[26] a) M. Bharathy, V. A. Rassolov, H.-C. zur Loye, *Chem. Mater.* **2008**, *20*, 2268; b) Y.-Y. Zhou, Z.-F. Qiu, M.-K. Lü, Q. Ma, A.-Y. Zhang, G.-J. Zhou, H.-P. Zhang, Z.-S. Yang, *J. Phys. Chem. C* **2007**, *111*, 10190; c) M. Bharathy, V. A. Rassolov, S. Park, H.-C. zur Loye, *Inorg. Chem.* **2008**, *47*, 9941.
[27] H.-Y. Zhu, Z.-F. Zheng, X.-P. Gao, Y.-N. Huang, Z.-M. Yan, J. Zou, H.-M. Yin, Q.-D. Zou, S. H. Kable, J.-C. Zhao, Y.-F. Xi, W. N. Martens, R. L. Frost, *J. Am. Chem. Soc.* **2006**, *128*, 2373.
[28] a) S. Nellutla, J. V. Tol, N. S. Dalal, L.-H. Bi, U. Kortz, B. Keita, L. Nadjo, G. A. Khitrov, A. G. Marshall, *Inorg. Chem.* **2005**, *44*, 9795; b) B. Keita, I. M. Mbomekalle, L. Nadjo, *Electrochem. Commun.* **2003**, *5*, 830; c) J.-Q. Sha, J. Peng, H.-S. Liu, J. Chen, B.-X. Dong, A.-X. Tian, Z.-M. Su, *Eur. J. Inorg. Chem.* **2007**, 1268; d) D. Jabbour, B. Keita, L. Nadjo, U. Kortz, S. S. Mal, *Electrochem. Commun.* **2005**, *7*, 841; e) L. Ruhlmann, L. Nadjo, J. Canny, R. Contant, R. Thouvenot, *Eur. J. Inorg. Chem.* **2002**, *4*, 975; f) B. Keita, E. Abdeljalil, L. Nadjo, B. Avisse, R. Contant, J. Canny, M. Richet, *Electrochem. Commun.* **2000**, *2*, 145.
[29] M. Filowitz, R. K. C. Ho, W. G. Klemperer, W. Shum, *Inorg. Chem.* **1979**, *18*, 93.
[30] a) H.-X. Ju, S.-Q. Liu, B.-X. Ge, F. Lisdat, F. W. Schellerb, *Electroanalysis* **2002**, *14*, 142; b) X.-L. Wang, N. Li, A.-X. Tian, J. Ying, D. Zhao, X.-J. Liu, *Inorg. Chem. Commun.* **2012**, *25*, 60.
[31] N. F. M. Henry, K. Lonsdale (Eds.), *International Tables for X-ray Crystallography*, Kynoch Press, Birmingham, UK, **1952**.
[32] G. M. Sheldrick, *SHELXL 97, Program for the Refinement of Crystal Structure*, University of Göttingen, Germany, **1997**.
Received: September 21, 2012
Published Online: February 28, 2013

